

## Evaporation Loss of Dissolved Volatile Substances from Ice Surfaces

Keiichi Sato,\*<sup>†</sup> Norimichi Takenaka, Hiroshi Bandow, and Yasuaki Maeda

Graduate School of Engineering, Osaka Prefecture University, 1-1, Gakuen-cho, Naka-ku, Sakai-City, Osaka 599-8531, Japan

Received: July 16, 2007; Revised Manuscript Received: May 29, 2008

Volatile acidic solutes were used to make dilute solutions, which were frozen by various methods. The concentration of solutes and the pH of the samples were measured before and after being frozen. When the sample solution is frozen from the bottom to the top, solutes are concentrated into the unfrozen solution (i.e., the upper part of the sample) due to the freeze concentration effect. Thereafter, concentrated anions combine with protons to form acids, and the amount of acids in the unfrozen solution increase as the ice formation progresses. At the end of freezing, the acid is saturated at the ice surface, and if the formed acid is volatile, then evaporation occurs. Frozen solutions were allowed to stand below 0 °C, where evaporation rates were obtained in the following order: formate > acetate > propionate > *n*-butyrate > chloride ≫ nitrate. Except for nitrate, evaporation rates were enough to take place in frozen water of the natural environment (e.g., ice crystal, graupel, snow crystal, and frozen droplets). The relationship between the evaporation rate of volatile acids and their physical properties demonstrate that the evaporation rates of weak acids are faster than those of strong acids, and the evaporation rates among weak acids are the same as the volatility of weak acids.

### Introduction

Freezing is commonly used to preserve substances in solution because their compositions are believed not to change in a freezing process. The main reasons for which chemical reactions are inhibited in a solid phase is that collisions of molecules are heavily suppressed. Some chemical reactions, however, are known to accelerate in partially frozen aqueous solutions.<sup>1–19</sup> Some possible mechanisms for acceleration by freezing have been summarized in the literature.<sup>9,20</sup> Fennema reported that the freeze-concentration effect, the concentration of solutes caused by exclusion from the tight bonding network of ice crystals, is considered to be the most important.<sup>9</sup> Our previous study also suggested that the acceleration of the oxidative reaction rate from nitrite to nitrate by freezing is induced by a rapid confinement of reactants in a small pocket between ice crystals.<sup>14</sup>

On the other hand, several reports have explained that a change in composition of some solutes during a freezing process was the result of electrochemical reactions, caused by the freezing potential, an electrical potential generating at the interface between aqueous solution and ice due to charge separation of ions in the two different phases. Lodge et al. reported that the chloride ion concentration decreased when a dilute sodium chloride aqueous solution was frozen and then thawed.<sup>21</sup> They explained that this decrease is associated with the freezing potential. Finnegan et al. also reported that decreases of various solutes including chloride ion associated with electrochemical reactions are attributable to the freezing potential.<sup>12</sup> However, there are many uncertain points in their suggesting electrochemical reactions. For example, most products of the reactions were not determined. In our previous study, the contribution of electrochemical reactions, induced by freezing, toward a change in composition was found to be negligible if such reactions actually occur.<sup>14</sup> Moreover, Lodge

et al.'s reported change in chloride ion concentration<sup>21</sup> has not been sufficiently explained.

Due to electrical imbalance in ice grown from an electrolyte solution, the pH of the unfrozen solution was reported to significantly change.<sup>19,22</sup> If an unfrozen solution deviates from its acid–base equilibrium state, a fraction of undissociated volatile acid in the unfrozen solution may escape to the gas phase. This study has demonstrated the freeze-concentration effect of solutes, the decrease in the concentration of solutes in a frozen–thawed sample due to the deviation of acid–base equilibrium state, and evaporation into the gas phase when a dilute aqueous solution was frozen by various methods. Furthermore, the respective decreasing rates of the following substances are discussed after the samples, doped with either chloride, nitrate, formate, acetate, propionate, or *n*-butyrate, were frozen and allowed to stand in a freezer. Nitrite is a compound that probably escapes from the surface of ice, but nitrite reacts rapidly with dissolved oxygen during a freezing process.<sup>14</sup> Therefore, it is hard to quantitatively evaluate the decreasing rate.

Finally, the possibility and implications of evaporative loss of volatile acids in the environment is discussed. Freezing is an ordinary occurrence in the environment that contributes significantly to various precipitation processes.<sup>23,24</sup> Recent studies demonstrate the quasi-liquid layer, which forms between ice and the gas phase, plays an important role on chemical behaviors in the atmosphere.<sup>25</sup> Taking into account its significance in the environment, it should be noted that the change in chemical composition of an aqueous solution in the freezing process may affect chemical compositions of a suite of substances, such as rain, fog, and snow.

### Experimental Section

**Experimental Procedure.** A dilute acidic solution (typical concentrations of solutes were 100 μM) of sodium chloride, sodium nitrate, sodium formate, sodium acetate, sodium propionate, or sodium *n*-butyrate was frozen by various methods.

\* To whom correspondence should be addressed. Phone: (+81)25-263-0562. Fax: (+81)25-263-0567. E-mail: ksato@adorc.gr.jp.

<sup>†</sup> Present address: Data Management Department, Acid Deposition and Oxidant Research Center, 1182 Sowa, Nishi-ku, Niigata, 950-2144, Japan.

After the samples were completely frozen, some samples were thawed immediately. Other samples stood in a freezer at  $-6\text{ }^{\circ}\text{C}$  to investigate a change in concentration with time. After the frozen samples were completely thawed, concentrations of solutes in the samples were measured. In the case of gas-phase measurements, substances evaporating from the frozen sample were collected by dissolving them into an alkaline solution. The number of moles of each ion contained in the frozen-thawed sample was compared to that in the original solution. When the concentrations of ions in ice and solution were analyzed separately, the solution part, which was open to the gas phase, was separated by removing it with a syringe, and then the remaining frozen part was thawed. Reproducibility could be confirmed by three repetitive experimental runs, and time profiles of ion concentrations in unfrozen solution, ice, and gas phase were attained by a set of different experimental runs. pH measurements for some of the ice or solution samples were carried out at room temperature. Ice samples were completely thawed prior to the pH measurement.

All reagent grade chemicals were obtained from Wako Pure Chemical Industries, Ltd., Osaka, Japan and used without further purification. Purified nitrogen gas (purity  $\geq 99.9999\%$ ), which was used for collecting the evaporating substances, was obtained from Taiyo Nippon Sanso. Aqueous solutions were prepared with ultra pure water (Simpli Lab-UV; Japan Millipore Co., Tokyo, Japan; resistivity  $\geq 18.2\text{ M}\Omega\text{ cm}$ ). The pH of solutions was adjusted with sulfuric acid prior to freezing.

Inorganic anions were determined by an IC-7000-type ion chromatographic analyzer (Yokogawa Analytical Systems, Inc., Tokyo, Japan; eluent solution,  $1\text{ mM NaHCO}_3$  and  $2.5\text{ mM Na}_2\text{CO}_3$ ; flow rate,  $1\text{ cm}^3\text{ min}^{-1}$ ) with an ICS-A23 column. Organic anions were determined by an IC-7000E-type ion chromatographic analyzer (Yokogawa Analytical Systems, Inc.; eluent solution,  $1\text{ mM H}_2\text{SO}_4$ ; flow rate,  $1\text{ cm}^3\text{ min}^{-1}$ ) with a CHA-E11 column. Sodium ions were determined by flame photometry (208 atomic absorption spectrophotometer, Hitachi, Ltd., Tokyo, Japan), and the pH of a sample solution was measured with a pH meter (CP-1 digital desktop pH meter, COS, Ltd., Kyoto, Japan; and SE-1700GC glass electrode, Fuji Chemical Measurement Co., Ltd., Tokyo, Japan), which was calibrated with pH 7 and 4 buffer solutions.

**Freezing Methods.** A sample solution was frozen by one of the following five methods. The basic idea of these methods is explained in detail in our previous work.<sup>14</sup> Only the special usage for this study is described below.

(i) Freezing from the surroundings: A  $15\text{ cm}^3$  volume of a sample solution was put in a Pyrex test tube, and the tube was immersed in a coolant. In this method, the sample was frozen from the surroundings to the center, and the interface of the sample and the gas phase was frozen before the whole sample was frozen. The sample was completely frozen within approximately 30 min.

(ii) Freezing from the bottom: A  $15\text{ cm}^3$  volume of a sample solution was put in a glass vessel of which the inner diameter and height were 35 mm and 72 mm, respectively. To prevent supercooling, the bottom of the vessel (5 mm height) was first immersed in liquid nitrogen for 15 s, and a thin ice film was formed before the freezing experiments. Subsequently, the bottom of the vessel was immersed in a coolant ( $-6\text{ }^{\circ}\text{C}$ ). The sample was frozen from the bottom to the top, and the interface of the sample and the gas phase was finally frozen within approximately 80 min.

(iii) Freezing from the bottom used for mass balance confirmation: This manner of freezing was the same as method

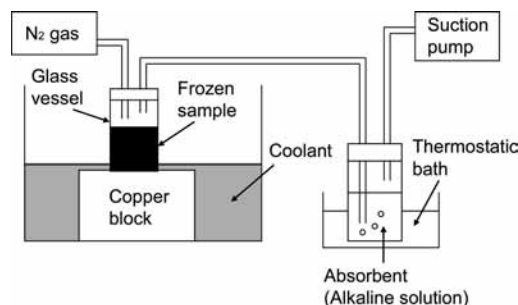


**Figure 1.** Experimental setup for freezing method (iii). The temperature of the coolant was adjusted to  $-6\text{ }^{\circ}\text{C}$ , and the thermostatic bath was adjusted to  $4\text{ }^{\circ}\text{C}$ . The flow rate of the suction pump was  $200\text{ cm}^3\text{ min}^{-1}$ .

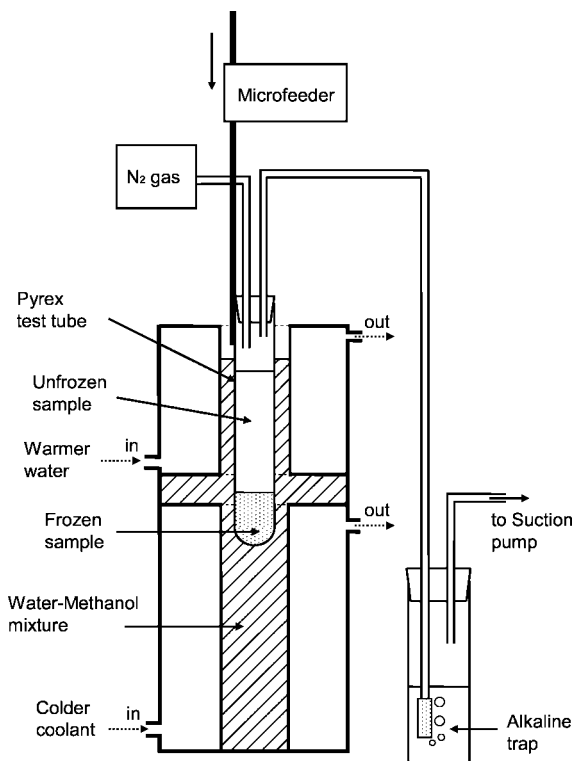


**Figure 2.** Freezing apparatus for freezing method (iv). The temperature of the warmer water was adjusted to  $5\text{ }^{\circ}\text{C}$ , and the colder coolant was adjusted to  $-5$  or  $-10\text{ }^{\circ}\text{C}$ . The flow rate of the suction pump was  $200\text{ cm}^3\text{ min}^{-1}$ .

ii. To investigate the amount of evaporated gas, the experimental setup shown in Figure 1 was employed. Purified nitrogen gas was introduced into the vessel, and the evaporated gas was flushed and then trapped into an alkaline solution. Concentrations of the substances trapped in the absorbent were analyzed at several hour intervals, and the evaporation amount from the sample was monitored.

(iv) Freezing from the bottom at a constant freezing speed: The freezing rate was not well-controlled in method (ii). To control the freezing rate, the sample was frozen using the apparatus shown in Figure 2. This apparatus consisted of three parts: the upper warmer zone, the middle window zone, and the lower colder zone. The temperature of the warmer zone was adjusted above the freezing point, and the colder zone was adjusted below the freezing point. Before the freezing experiment,  $15\text{ cm}^3$  of the sample solution was put in a Pyrex test tube of which the inner diameter and height were 15 mm and 180 mm, respectively. Then the bottom of the test tube was immersed in liquid nitrogen for 15 s. The test tube was moved

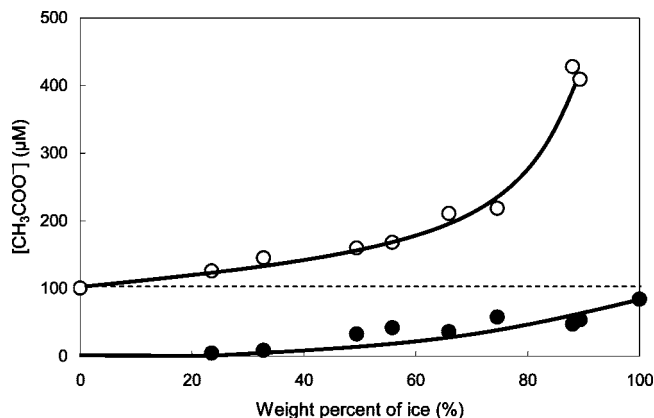


**Figure 3.** Changes in acetate concentration in the ice and unfrozen solution versus the progression of ice formation using the freezing method (iv): ●, ice; ○, unfrozen solution. Additional conditions:  $[\text{CH}_3\text{COONa}]_0$ , 100.0  $\mu\text{M}$ ;  $\text{pH}_0$ , 4.25; sample volume, 15.0  $\text{cm}^3$ . The broken line indicates the initial concentration. Weight percent (%) of ice = weight of the frozen part (g)/weight of the entire bulk sample (g).

down slowly at a constant rate (4.5–6.25 mm/h) with a microfeeder in order to freeze the sample from the bottom. When freezing was carried out in this way, the interface of the ice and the solution appeared in the middle window zone. The freezing rate was the same as the transfer rate of the microfeeder. The gas-phase measurement apparatus was the same as that in method iii.

(v) Freezing in vessels having various bottom areas: A 15  $\text{cm}^3$  volume of the sample solution was put in glass beakers with bottoms that varied in area (5.68–92.6  $\text{cm}^2$ ), and the bottoms of these beakers (several millimeters thickness) were buried outdoors in the ground. The outdoor temperature ranged from  $-3.2$  to  $-8.5$   $^\circ\text{C}$  during these experiments. The entire sample was completely frozen in approximately 120 min after the beakers were left outside, which were then kept outside for 13 h.

In freezing methods (i), (ii), and (v), an aluminum foil was used to cover the mouth of the vessel in order to prevent external contaminations. However, the mouth was not tightly sealed, and thus the experimental system was possibly open to the gas phase.

## Results and Discussion

**Freeze-Concentration Effect and Evaporation Mechanism of Volatile Solutes.** To investigate the freeze-concentration effect, 100.0  $\mu\text{M}$  sodium acetate solution was frozen by method (iv), and time variations of acetate concentration in ice and unfrozen solution were measured. The results are shown in Figure 3. The fitting curves shown hereinafter were depicted by smooth fitting. Since the ice formed was polycrystalline, small amounts of acetates were confined into grain boundaries and thus detected in the ice. On the other hand, the majority of acetates were excluded from the ice and concentrated in the unfrozen solution, where the concentration of acetates in the unfrozen solution increased with the progression of ice formation. When 90% of the sample was frozen, acetate ions were concentrated by approximately 4 times compared to the initial concentration. In method (iv), the concentration of acetate in the unfrozen solution could not be measured just before the sample was completely frozen. However, the results of Figure 3 clearly demonstrate that acetates were concentrated at the surface of the sample (i.e., the acetate concentration at the surface is expected to be very high).

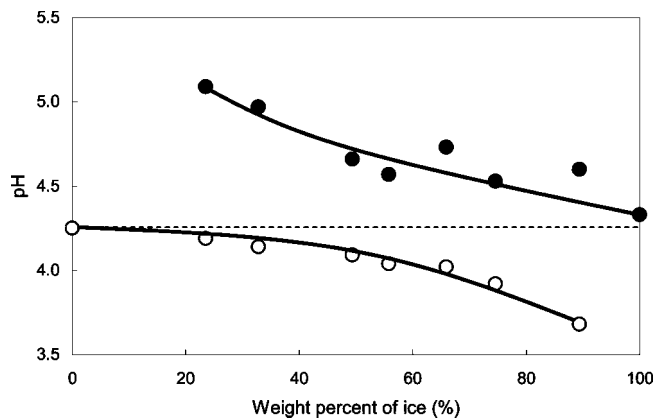


**Figure 4.** Changes in the pH of ice and unfrozen solution with the progression of ice formation using freezing method (iv): ●, ice; ○, unfrozen solution. Additional conditions:  $[\text{CH}_3\text{COONa}]_0$ , 100.0  $\mu\text{M}$ ;  $\text{pH}_0$ , 4.25; sample volume, 15.0  $\text{cm}^3$ . The pH measurements were carried out at room temperature. The broken line indicates the initial pH. Weight percent (%) of ice = weight of the frozen part (g)/weight of the entire bulk sample (g).

The respective pH values of the ice and the solution parts were also measured. Figure 4 shows time variations of the pH of the ice and the solution parts. The pH of the solution dropped below the initial value. When the sodium acetate solution was frozen, both acetate and sodium ions were concentrated into the unfrozen solution due to the freeze-concentration effect. In this experimental system, sulfuric acid was used for pH adjustment, and sulfates were also concentrated into the unfrozen solution. The distribution coefficients of acetate and sulfate ions in ice are both lower than that of sodium ions.<sup>26</sup> Therefore, the negative potential should generate in the unfrozen solution. This generated freezing potential is then neutralized by the movement of highly mobile protons from the ice to the unfrozen solution, and the pH of the unfrozen part of the solution eventually drops below the initial value. This result supports recent findings by Robinson et al. that showed that the preferential segregation of anions to the unfrozen solution of ice matrices will lower the pH of the unfrozen solution after temperature equilibration and charge neutralization.<sup>22</sup> Because of deviation from the equilibrium state of acetic acid, it is assumed that the concentrated acetates combine with the migrated protons to form  $\text{CH}_3\text{COOH}$  and that the undissociated acetic acid in the unfrozen solution will increase as the ice formation progresses. At the end of the freezing, the undissociated acetic acid will be saturated at the surface.

If the freezing temperature is below the eutectic temperature of the  $\text{CH}_3\text{COONa}-\text{H}_2\text{SO}_4-\text{H}_2\text{O}$  system, all components in the frozen sample should solidify. In this case, evaporation of substances induced by supersaturation in the frozen solution should not occur. The eutectic point of the  $\text{CH}_3\text{COOH}-\text{H}_2\text{O}$  system is  $-27$   $^\circ\text{C}$ , and that of the  $\text{H}_2\text{SO}_4-\text{H}_2\text{O}$  system is  $-73$   $^\circ\text{C}$ .<sup>27,28</sup> Those temperatures are much lower than the freezing temperature ( $-6$   $^\circ\text{C}$ ). The eutectic points of the binary systems of  $\text{CH}_3\text{COONa}-\text{H}_2\text{O}$  and  $\text{Na}_2\text{SO}_4-\text{H}_2\text{O}$  and the ternary system of  $\text{CH}_3\text{COONa}-\text{H}_2\text{SO}_4-\text{H}_2\text{O}$  are not available but are also expected to be much lower than  $-6$   $^\circ\text{C}$ . Consequently, solidification in the eutectic system might not give a significant effect on this experimental system. On the other hand, Boxe et al. reported the presence of subeutectic microscopic solutions during pure desorption experiments at temperatures as low as  $-30$   $^\circ\text{C}$  for ice samples containing micromolar amounts of  $\text{NaNO}_3$  ( $T_{\text{eutectic}} = -18$   $^\circ\text{C}$ )<sup>29</sup> and also reported gases had been

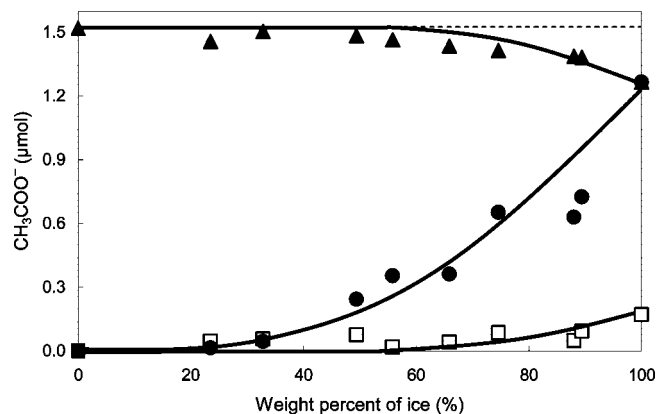


**Figure 5.** Changes in the number of moles of acetate in ice, unfrozen solution, and gas phase with the progress of ice formation in freezing method (iv): ●, ice; ▲, ice + unfrozen solution; □, gas phase. Additional conditions:  $[\text{CH}_3\text{COONa}]_0$ , 100.0  $\mu\text{M}$ ;  $\text{pH}_0$ , 4.25; sample volume, 15.0  $\text{cm}^3$ . The broken line indicates the initial number of moles of acetate in the sample. Weight percent (%) of ice = weight of the frozen part (g)/weight of the entire bulk sample (g).

detected below the eutectic temperature.<sup>29–31</sup> Further investigation below the eutectic points will be necessary.

The number of moles of acetate ion in the ice, unfrozen solution, and the gas phase can be calculated from the solute concentrations shown in Figure 3 and weights of ice, solution, and alkaline solution. Figure 5 shows time variations of the number of moles of acetate ion in freezing method (iv). The total amount of acetate in the ice and in the unfrozen solution decreased, whereas that in the gas phase increased as the ice formation progressed. When the whole sample was completely frozen, the decrease in the number of moles of acetate in the sample was 234 nmol, and that of acetate detected in the gas phase was 171 nmol. The mass balance of acetate was not good. Since the acetate concentration in the second alkaline trap which was set behind the first trap in some cases was below the detection limit (0.1 nmol), all evaporated acetates introduced into the alkaline trap could be collected. The most probable reason of this mass balance discrepancy is lost in the transfer tube which was connected into the alkaline trap (Figure 2). On the basis of the results from Figure 3 and Figure 5, it is assumed that acetate was concentrated into the surface of the ice and that the formed  $\text{CH}_3\text{COOH}$  evaporated into the gas phase when the sample had been frozen from the bottom.

The manner of the freeze concentration will be strongly affected by the manner of ice formation based on the result of Figure 3. To investigate how a particular method of freezing affects the composition of a sample solution, 100  $\mu\text{M}$  sodium acetate or sodium chloride solution was frozen using methods (i) and (ii) and then thawed immediately thereafter. As shown in Table 1, when both samples were frozen from the surroundings (method (i)), acetates or chlorides were concentrated in the center of the sample and confined there; thus, they were difficult to escape into the gas phase. Consequently, a substantial change of acetate or chloride ion concentration was not observed after the sample was frozen and then thawed. On the other hand, when both samples were frozen from the bottom (method (ii)), acetates or chlorides were concentrated into the ice surface, and the formed  $\text{CH}_3\text{COOH}$  or  $\text{HCl}$  could evaporate from the surface to the gas phase. Therefore, the concentrations of acetate and chloride in the frozen–thawed samples decreased. Comparison of the pH values of unfrozen sample (i.e., the initial pH of the solution prior to freezing) and the frozen–thawed sample are also shown in Table 1. In the case of freezing from the bottom,

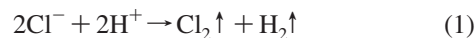
**TABLE 1: Comparison of the Concentrations of Anions after Freezing and the pH Values between Freezing Methods (i) and (ii)<sup>a</sup>**

anion	freezing method	concentrations after freezing ( $\mu\text{M}$ )	initial pH	pH after freezing
acetate	(i)	98.1	3.00	3.00
		100.7	4.75	4.75
	(ii)	101.3	5.35	5.35
		87.8	3.00	3.00
chloride	(i)	95.0	4.75	4.81
		100.7	3.50	3.50
	(ii)	91.9	4.00	4.12
		93.7	4.25	4.39
		94.5	4.50	4.60
		97.2	4.75	4.88

<sup>a</sup> Initial  $\text{CH}_3\text{COONa}$  or  $\text{NaCl}$  concentration was 100.0  $\mu\text{M}$ .

the concentrations of anions decreased, and the pH of the sample increased after freezing. On the other hand, in the case of freezing from the surroundings, no changes in the concentrations of anions and the pH value were observed. These results show that  $\text{CH}_3\text{COOH}$  or  $\text{HCl}$ , which is formed by bonding acid constituents and protons, evaporates into the gas phase, and thus the concentrations of acid constituent and proton decrease simultaneously. As a result, the pH of the sample increases due to the eventual evaporation of the acids.

In the case of chloride, the electrochemical reaction by the freezing potential, that is,



was reported.<sup>12,21</sup> The value of the freezing potential is reported to be  $-90$  to  $+214$  V.<sup>26</sup> Such a high electrochemical potential seems to be sufficient to allow most reactions to occur. However, we previously noted that the amounts of the products produced by the electrochemical reaction depend on a consumed electric current, where the current obtained in the freezing process is dominated by the number of ions separated into the bulk ice and unfrozen solution.<sup>14</sup> To achieve an efficient reaction, the separated ions must react efficiently without relaxation by another process, such as neutralization by transfer of protons. Furthermore, the freezing potential is created by the freezing process, rather than a frozen sample.<sup>26</sup> In addition, there are some ambiguous points in the reported electrochemical reactions due to freezing. For example, the products detected in the electrochemical reaction could not be clearly defined.<sup>12</sup> Furthermore, when 100  $\mu\text{M}$  sodium chloride solution was kept in a container which is the same type as Lodge et al. used<sup>21</sup> for 24 h, 7.2% of chloride was adsorbed on the surface of the copper plate. In our experiments, after thawing, the increase in pH of the frozen sample and the decrease in the concentration of chloride were primarily caused by the evaporation of volatile acid, such as hydrochloric acid from the ice surface, and not by the electrochemical reaction.

The results shown in Table 1 demonstrate the other important feature. The loss amounts of acetates and chloride decreased with increasing the initial pH. At lower pH region ( $\text{pH} < \text{p}K_a$ ), weak acids such as acetic acid mainly exist as neutral compounds. As pH value increases, the weak acids will dissociate into ions, and the amount of the undissociated acids in the sample will decrease. If an alkaline solution is frozen, all of the acids will dissociate, and the evaporation cannot occur. In the case of the strong acids such as hydrochloric acid, the weaker dependence of the pH value on the amount of loss of solutes was observed. In this case, most of the solutes exist as



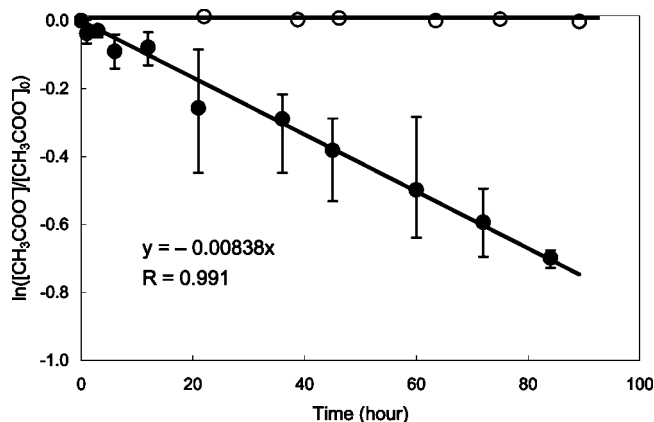


**Figure 6.** Time profile of acetate concentration in frozen sample and unfrozen solution: ●, frozen sample ( $-6\text{ }^{\circ}\text{C}$ ); ○, unfrozen solution ( $5\text{ }^{\circ}\text{C}$ ). Additional conditions:  $[\text{CH}_3\text{COONa}]_0$ ,  $100.0\text{ }\mu\text{M}$ ;  $\text{pH}_0$ , 4.00; sample volume,  $15.0\text{ cm}^3$ . Samples were frozen by freezing method ii and allowed to stand in a freezer ( $-6\text{ }^{\circ}\text{C}$ ). Time zero is defined as the time when the whole sample was completely frozen. Error bars show the highest and the lowest values ( $n = 3$ ).

dissociated ions in an acidic condition. Therefore, other factors (e.g., the interaction of solute and  $\text{H}_2\text{O}$ ) may affect the amount of evaporation. Chemical analysis of cloudwater collected by aircraft over the Japan Sea and the northwestern Pacific Ocean demonstrated that pH of cloudwater was within the range of 3.8–5.0.<sup>32</sup> The result of Table 1 demonstrates that a decrease in solute concentration is likely to take place in the pH region of cloudwater.

**Evaporation Rate from the Ice Surface.** The sodium acetate solution was frozen by method (ii) and allowed to stand at a constant temperature at  $-6\text{ }^{\circ}\text{C}$ . The time profile of the ion concentration change was investigated. Figure 6 shows the time variation of the acetate concentration change when  $100.0\text{ }\mu\text{M}$  sodium acetate solution was frozen and allowed to stand at  $-6\text{ }^{\circ}\text{C}$ . As mentioned above, when a sodium acetate solution is frozen from the bottom, most acetates are concentrated on the ice surface in which acetic acid forms. This figure demonstrates that the concentration of acetate decreased with the preserving time in a freezer. The decrease of acetate concentration obeyed first-order kinetics with respect to acetate concentration in the bulk sample. The rate constant of the first-order decay was  $8.38 \times 10^{-3}\text{ h}^{-1}$ . This figure also demonstrates the time profile for the unfrozen solution that stood at  $5\text{ }^{\circ}\text{C}$  showed no change in acetate concentration. Therefore, the decrease at  $-6\text{ }^{\circ}\text{C}$  was not due to microorganisms or to evaporation from the solution. Furthermore, it is apparent that the decrease from the frozen sample was much more than that in the course of the freezing process.

As mentioned previously, the quasi-liquid layer plays an important role on chemical behaviors in the atmospheric environment. Bluhm et al. investigated the relationship between the thickness of the quasi-liquid layer and the temperature of pure ice.<sup>33</sup> The temperature of ice was higher; the quasi-liquid layer was thicker. The quasi-liquid layer was not observed below  $-25\text{ }^{\circ}\text{C}$ . Therefore, the freezing temperature may affect the amount of undissociated acids on the ice surface. We carried out the following experiment;  $100.0\text{ }\mu\text{M}$  sodium acetate solution was frozen by method (ii), and then the frozen sample was allowed to stand at various temperatures ( $-1$ ,  $-3$ ,  $-5$ ,  $-7$ ,  $-9$ ,  $-11$ ,  $-13$ , and  $-15\text{ }^{\circ}\text{C}$ ) for 24 h. At higher than  $-3\text{ }^{\circ}\text{C}$ , the loss of acetates was only slight ( $<2.0\text{ }\mu\text{M}$ ), while the loss of acetates was more in the range of  $4.0$ – $6.0\text{ }\mu\text{M}$  from  $-5$  to  $-15\text{ }^{\circ}\text{C}$ . At higher ice temperature, the volume of the quasi-liquid

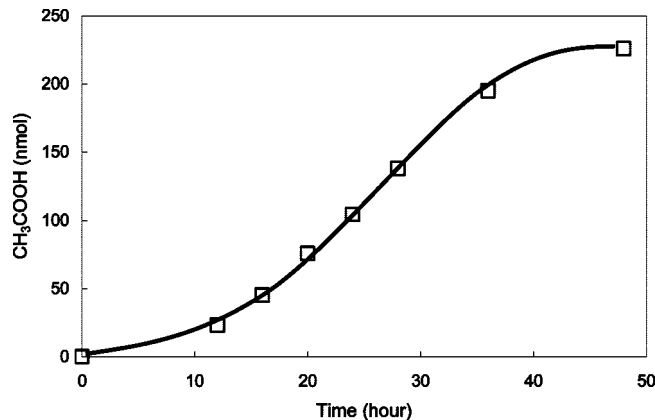


**Figure 7.** Time profile of the amount of acetate evaporated:  $[\text{CH}_3\text{COONa}]_0$ ,  $100.0\text{ }\mu\text{M}$ ;  $\text{pH}_0$ , 4.00; sample volume,  $15.0\text{ cm}^3$ . The samples were frozen by freezing method (iii) and allowed to stand in a freezer ( $-6\text{ }^{\circ}\text{C}$ ). Time zero is defined as the time when the whole sample was completely frozen.

layer is larger, and thus the amount of undissociated acid to the gas phase would be small. Although similar experiments below  $-15\text{ }^{\circ}\text{C}$  were not carried out, evaporation of volatile acids will be hard to occur at low temperature because the quasi-liquid layer does not exist at pure ice temperatures below  $-25\text{ }^{\circ}\text{C}$ .

In addition to the above observation, the amount evaporated to the gas phase was also measured using method iii. Figure 7 shows the time profile of the amount of the acetate detected in the gas phase. This result demonstrates that the amount of evaporated acetate increased sigmoidally with the standing time. Although there is an inconsistency between the decrease pattern in acetate concentration and the increase pattern in the evaporation amount, the amount of acetate detected in the gas phase was  $226.0\text{ nmol}$  for 48 h, which was almost the same amount of acetate decreased from the sample ( $220.8\text{ nmol}$ ). This result also supports the idea that the acetic acid formed on the ice surface will gradually evaporate to the gas phase.

For other organic acids such as formic, propionic, and *n*-butyric acids and inorganic acids such as hydrochloric and nitric acids, the same experiments as those for acetate were carried out. From those experiments, first-order decay profiles in solute concentration similar to that for acetate were observed. Figure 8 shows the time profiles of each anion concentration change when a sodium formate, sodium propionate, sodium *n*-butyrate, sodium chloride, or sodium nitrate solution was frozen by method (ii) and allowed to stand at a constant temperature ( $-6\text{ }^{\circ}\text{C}$ ). The first-order rate constants for formate, propionate, *n*-butyrate, and chloride concentrations were  $2.13 \times 10^{-2}$ ,  $5.20 \times 10^{-3}$ ,  $2.67 \times 10^{-3}$ , and  $1.47 \times 10^{-3}\text{ h}^{-1}$ , respectively. No loss was observed for nitrate in this particular experiment. The fact that almost the same profiles among the investigated substances were obtained implies that the evaporation mechanisms of the other acidic substances are the same as that of acetate, namely, the concentrated anion combines with the proton to form acid such as formic acid, propionic acid, *n*-butyric acid, or hydrochloric acid. The amounts of undissociated acid in the unfrozen solution increase with the progression of ice formation. At the end of each freezing period, the undissociated acid is saturated at the ice surface. Thereafter, acids will begin to evaporate if the acid formed is volatile.

If the acid formed at the surface of the frozen sample is volatile, the ratio of surface area to sample volume may affect the decrease of a solute from the frozen sample. A constant

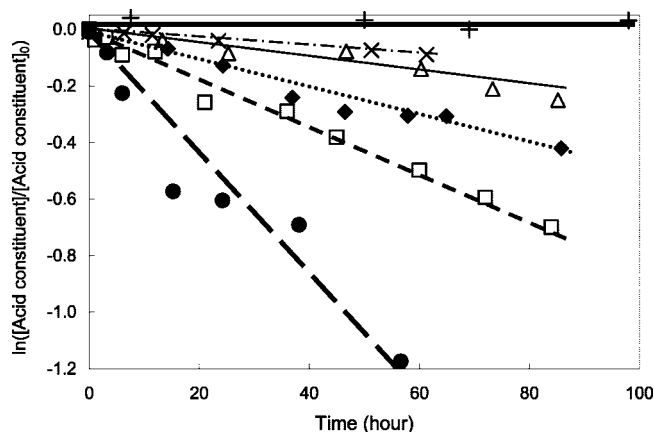


**Figure 8.** Time profiles of respective acid constituent concentrations in frozen samples: ●, formate; □, acetate; ◆, propionate; △, *n*-butyrate; ×, chloride; +, nitrate. Each sample solution was frozen by freezing method (ii) and allowed to stand in a freezer ( $-6\text{ }^{\circ}\text{C}$ ). Each initial solute concentration was  $100.0\text{ }\mu\text{M}$ , with  $\text{pH}_0\text{ }4.00$  and sample volume of  $15.0\text{ cm}^3$ . Time zero is defined as the time when the whole sample was completely frozen.

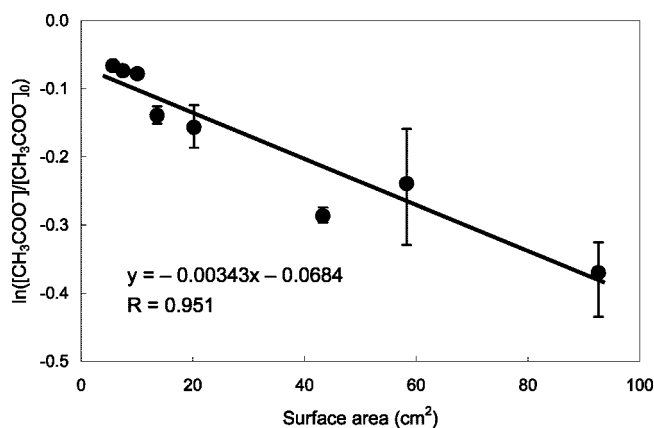


**Figure 9.** Change in acetate ion concentration in the course of freezing with various surface areas:  $[\text{CH}_3\text{COONa}]_0$ ,  $100.0\text{ }\mu\text{M}$ ;  $\text{pH}_0$ ,  $4.00$ ; sample volume,  $15.0\text{ cm}^3$ ; outdoor temperature,  $-3.2$  to  $-8.5\text{ }^{\circ}\text{C}$ . Samples were frozen outdoors for  $13\text{ h}$ . Error bars show the highest and the lowest values ( $n = 3$ ).

volume ( $15\text{ cm}^3$ ) of sodium acetate solution was frozen by method v, and the effect of the ratio of the surface area to the sample volume was investigated. The results are shown in Figure 9. The loss of acetate increased linearly with increasing the surface area. Kawamura and Mackey reported dependence of evaporation rate on liquid surface area in an opened system.<sup>34</sup> The evaporation rate was estimated by available physicochemical properties and expressed by the following equation.

$$E = AK_m(M_w P_v)/(RT) \quad (2)$$

where  $E$ ,  $A$ ,  $K_m$ ,  $M_w$ ,  $P_v$ ,  $R$ , and  $T$  denote evaporation rate, liquid surface area, mass-transfer coefficient of solutes, molecular weight of solute, vapor pressure of solute, the gas constant, and ambient temperature, respectively. There is a limitation with respect to the mass-transfer coefficient of solutes because movement of solute in the frozen sample was suppressed. Therefore, in consideration of the eq 2, the surface area is assumed to be the determinant of the evaporation rate. These results also support the idea that the volatile acid will evaporate from the ice surface.

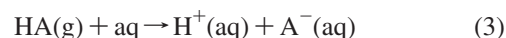
In method (v), the bottom part of a glass beaker was placed inside the ground, and thus the bottom was cooled faster than the sample solution. Therefore, it is confirmed that the sample was

first frozen from the surroundings of the sample and then the surface of the sample was frozen finally. That is to say, the manner of freezing in method (v) is similar to that in methods (ii)–(iv). Therefore, solutes are expected to evaporate in freezing method (v). This manner of freezing often happens in nature.<sup>23</sup> During immersed freezing nucleation, a small droplet is cooled by the cooling air around it, which is followed by rising in an updraft. If an ice nucleus is inside the droplet, ice can form around the embedded ice embryos. This contribution to the chemical compositions of actual clouds and precipitation has not been quantified for the moment. However, in view of the manner of freezing in nature, evaporation from the ice surface will cause the decrease in the concentration of some volatile anion species.

From the obtained results, each evaporation rate constant for various solutes can be calculated, and the residence times of solutes in a small spherical piece of ice can be estimated. The calculated results are summarized in Table 2. It takes 2–40 min to lose 10% of the investigated anion species from a spherical piece of ice with a diameter of  $10\text{ }\mu\text{m}$ . The diameters of fog and cloud droplets were reported to be in the range of several micrometers to a few tens of micrometers.<sup>23,38</sup> It takes several hours for rain or fog to form and precipitate on the ground.<sup>23</sup> Judging from the results in Table 2, the evaporation rates of the investigated volatile acids are enough to take place in the natural environment (e.g., ice crystal, graupel, snow crystal, and frozen droplets).

Some physical constants of the acids are also shown in Table 2. Among these substances, the evaporation rate was found as the following order: formate > acetate > propionate > *n*-butyrate > chloride  $\gg$  nitrate. It is well-known that solubilities of any solutes in ice are much lower than those in liquid water. This is due to the difficulty of incorporating the solute into the structured ice lattice compared to water, and thus anions are expected to attract neighboring protons to form undissociated acid, and the formed acid evaporates. Therefore, the evaporation must be dominated mainly by low acid dissociation constants (such as weak acids) and secondarily by boiling points or vapor pressures. Considering the physical constants of the acids, the difference in the evaporation rates of solutes between forming a strong acid and a weak acid is most likely due to the differences in the acid dissociation constants, and the differences in the evaporation rates among weak acids are probably due to differences in their vapor pressures. No nitrate loss was observed in our study. It is assumed that this observation is attributable to the large Henry's law constant of nitrate compared to that of chloride. Many researches reported that nitrate in ice undergoes photolysis and conversion into NO and NO<sub>2</sub> in laboratory studies.<sup>29–31,39,40</sup> Therefore, the escape of nitrate from ice is dominantly due to photolysis compared with the evaporation induced by the freeze-concentration effect.

Each above-mentioned physical constants will relate the volatility of solutes. Other factors, such as affinity of the acids and H<sub>2</sub>O, may be also related because enough energy to exceed the hydration force is required to evaporate to the gas phase. The following discussion deals with the standard enthalpy of formation of a hydrated ion when acid gas (HA) was dissolved in water. The hydration of acid gas can be explained as follows:



If 1 mol of the acid is dissolved in water at  $10^5\text{ Pa}$  and  $25\text{ }^{\circ}\text{C}$ , the standard enthalpy of formation of hydrated ion can be calculated in the equation below:

$$\Delta H_{\text{m,f}}^{\circ}[\text{H}^+(\text{aq}) + \text{A}^-(\text{aq})] = \Delta H^{\circ} + \Delta H_{\text{m,f}}^{\circ}[\text{HA}(\text{g})] \quad (4)$$

where  $\Delta H^{\circ}$  and  $\Delta H_{\text{m,f}}^{\circ}$  denote the enthalpy of solution and the standard enthalpy of formation, respectively. We can obtain the

**TABLE 2: Calculated Evaporation Rate Constants and Some Physical Constants of Acids**

solute	first-order rate constant per specific surface area ( $\text{h}^{-1} \text{cm}$ )	residence lifetime in spherical ice (s)			$K_a$ of acids <sup>b</sup>	vapor pressure <sup>c</sup> (kPa)	Henry's law constants <sup>d</sup> ( $\text{M atm}^{-1}$ )
		100 $\mu\text{m}$ <sup>a</sup>	50 $\mu\text{m}$ <sup>a</sup>	10 $\mu\text{m}$ <sup>a</sup>			
formate	$1.10 \times 10^{-3}$	$1.10 \times 10^4$	$5.48 \times 10^3$	$1.10 \times 10^3$	$1.64 \times 10^{-4}$ <sup>f</sup>	5.56	$5.53 \times 10^3$ <sup>h</sup>
acetate	$4.31 \times 10^{-4}$	$2.78 \times 10^4$	$1.39 \times 10^4$	$2.78 \times 10^3$	$1.66 \times 10^{-5}$ <sup>f</sup>	2.11	$5.50 \times 10^3$ <sup>h</sup>
propionate	$2.68 \times 10^{-4}$	$4.49 \times 10^4$	$2.24 \times 10^4$	$4.49 \times 10^3$	$1.27 \times 10^{-5}$ <sup>f</sup>	0.569	$5.64 \times 10^{-3}$ <sup>h</sup>
<i>n</i> -butyrate	$1.37 \times 10^{-4}$	$8.74 \times 10^4$	$4.37 \times 10^4$	$8.74 \times 10^3$	$1.56 \times 10^{-5}$ <sup>f</sup>	0.152	$4.55 \times 10^{-3}$ <sup>f</sup>
chloride	$7.56 \times 10^{-5}$	$1.59 \times 10^5$	$7.93 \times 10^4$	$1.59 \times 10^4$	$1.4 \times 10^7$ <sup>g</sup>	$4.76 \times 10^3$	1.1 <sup>g</sup>
nitrate	ND <sup>e</sup>	NA	NA	NA	16.0 <sup>g</sup>	7.52	$2.6 \times 10^6$ <sup>g</sup>

<sup>a</sup> Diameters of spherical ice. <sup>b</sup> Acid dissociation constants at 0 °C (except for nitrate at 25 °C). <sup>c</sup> Vapor pressures of acids at 25 °C.<sup>27</sup> <sup>d</sup> Henry's law constants of acids at 25 °C. <sup>e</sup> Decrease of ion was not detected for 72 h. <sup>f</sup> From Lide.<sup>27</sup> <sup>g</sup> from Nair et al.<sup>35</sup> <sup>h</sup> from Brimblecombe et al.<sup>36</sup> and Kahn et al.<sup>37</sup>

standard enthalpy of formation of a hydrated ion using the data of the enthalpy of solution and the standard enthalpy of the formation of the respective acid gas.<sup>27</sup> The standard enthalpies of the formation of hydrated formate, hydrated acetate, hydrated chloride, and hydrated nitrate are  $-425.43$ ,  $-278.95$ ,  $-167.16$ , and  $-168.30$   $\text{kJ mol}^{-1}$ , respectively. The hydrated organic acid anion has a larger energy potential than the hydrated inorganic acid anion, and thus the organic acid gas is expected to evaporate more readily than inorganic gas. Although many of the behaviors of solutes in ice have not been clarified yet, the above discussion suggests that the standard enthalpy of formation of hydrated solutes would affect the amount of solutes evaporated.

## Conclusions

This study elucidates that the evaporative loss of volatile substances from ice surfaces is mainly attributable to the freeze-concentration effect. A particular manner of freezing affects the evaporation amount from a frozen sample. When the surface of a sample is finally frozen, both solutes and protons are concentrated into the unfrozen upper part due to the freeze-concentration effect. As the ice formation progresses, a concentrated anion combines with a proton to form an acid. At the end of freezing, depending on the freezing method used, the acid is saturated at the ice surface, and if the acid formed is volatile, it evaporates. This observation does not apply to an alkaline solution because all the formed acids dissociate.

When a sample solution was frozen using the above-mentioned method and stood in a freezer, solutes gradually escape from the frozen sample. The decrease of acetate concentration obeyed first-order kinetics with respect to acetate concentration in the bulk sample. Respective evaporation rates of various volatile solutes from the ice surface were examined. It takes 2–40 min to lose 10% of the investigated anion species from a spherical piece of ice with a diameter of 10  $\mu\text{m}$ . These results suggest that the evaporation of solutes is expected to also take place in the natural environment. Some physical properties (e.g., state a few of the physical properties) of the volatile acids were found to affect the evaporation rate. The difference in evaporation rates of solutes between forming a strong acid and a weak acid is most likely due to the differences in the acid dissociation constants, namely, the amounts of the undissociated volatile acids at the ice surface. The difference in the evaporation rates among weak acids are probably due to differences in their vapor pressures that correspond to volatility of the acids. The obtained data demonstrated that the evaporation rate is dominated mainly by the acid dissociation constants and secondarily by vapor pressures.

It has been demonstrated that constituents in polar ice cores may change due to migration in the interstitial liquid that separate grain boundaries or molecular diffusion of trapped gas

in ice cores<sup>41,42</sup> or even slightly change due to photochemistry shown by McCabe et al.<sup>43</sup> These observations must be taken into consideration to derive the earth's paleoatmosphere from polar ice cores. In addition to these observations, the observed aging effect of ice as shown in this study has a significant impact for ice core samples stored for long periods of time.

**Acknowledgment.** This work was supported in part by a Grant-in-Aid for Scientific Research (C) (Grant No. 07680561) from The Ministry of Education, Science, Sports and Culture, Japan.

## References and Notes

- Grant, N. H.; Clark, D. E.; Alburn, H. E. *J. Am. Chem. Soc.* **1961**, *83*, 4476–4477.
- Bruice, T. C.; Butler, A. R. *J. Am. Chem. Soc.* **1964**, *86*, 4104–4108.
- Butler, A. R.; Bruice, T. C. *J. Am. Chem. Soc.* **1964**, *86*, 313–319.
- Weatherburn, M. W.; Logan, J. E. *Clin. Chim. Acta* **1964**, *9*, 581–584.
- Alburn, H. E.; Grant, N. H. *J. Am. Chem. Soc.* **1965**, *87*, 4174–4177.
- Grant, N. H.; Alburn, H. E. *Biochemistry* **1965**, *4*, 1913–1916.
- Grant, N. H.; Alburn, H. E. *Nature* **1966**, *212*, 194.
- Pincock, R. E. *Acc. Chem. Res.* **1969**, *2*, 97–103.
- Fennema, O. In *Water Relations of Foods*; Duckworth, R. B., Ed.; Academic Press: London, 1975; pp 539–556.
- Hatley, R. H. M.; Frank, F.; Day, H.; Byth, B. *Biophys. Chem.* **1986**, *24*, 41–46.
- Hatley, R. H. M.; Frank, F.; Day, H. *Biophys. Chem.* **1986**, *24*, 187–192.
- Finnegan, W. G.; Pitter, R. L.; Young, L. G. *Atmos. Environ.* **1991**, *25A*, 2531–2534.
- Takenaka, N.; Ueda, A.; Maeda, Y. *Nature* **1992**, *358*, 736–738.
- Takenaka, N.; Ueda, A.; Daimon, T.; Bandow, H.; Dohmaru, T.; Maeda, Y. *J. Phys. Chem.* **1996**, *100*, 13874–13884.
- Honda, K. *Nippon Kagaku Kaishi* **1997**, 717–719.
- Betterton, E. A.; Anderson, D. J. *J. Atmos. Chem.* **2001**, *40*, 171–189.
- Takenaka, N.; Furuya, S.; Sato, K.; Bandow, H.; Maeda, Y.; Furukawa, Y. *Int. J. Chem. Kinet.* **2003**, *35*, 198–205.
- Sato, K.; Furuya, S.; Takenaka, N.; Bandow, H.; Maeda, Y.; Furukawa, Y. *Bull. Chem. Soc. Jpn.* **2003**, *76*, 1139–1144.
- Takenaka, N.; Tanaka, M.; Okitsu, K.; Bandow, H. *J. Phys. Chem. A* **2006**, *110*, 10628–10632.
- Bronsteyn, V. L.; Chernov, A. A. *J. Cryst. Growth* **1991**, *112*, 129–145.
- Lodge, J. P.; Baker, M. L.; Pierrard, J. M. *J. Chem. Phys.* **1956**, *24*, 716–719.
- Robinson, C.; Boxe, C. S.; Guzman, M. I.; Colussi, A. J.; Hoffmann, M. R. *J. Phys. Chem. B* **2006**, *110*, 7613–7616.
- Young, K. C. *Microphysical Processes in Clouds*; Oxford University Press: Oxford, U.K., 1993.
- Takenaka, N.; Daimon, T.; Ueda, A.; Sato, K.; Kitano, M.; Bandow, H.; Maeda, Y. *J. Atmos. Chem.* **1998**, *29*, 135–150.
- Carignano, M. A.; Shepson, P. B.; Szleifer, I. *Chem. Phys. Lett.* **2007**, *436*, 99–103.
- Cobb, A. W.; Gross, G. W. *J. Electrochem. Soc.* **1969**, *116*, 796–804.
- Lide, D. R. *CRC Handbook of Chemistry and Physics*, 87rd ed.; CRC Press: New York, 2006.

- (28) Price, P. B. *Proc. Natl. Acad. Sci. U.S.A.* **2000**, *97*, 1247–1251.
- (29) Boxe, C. S.; Colussi, A. J.; Hoffmann, M. R.; Murphy, J. G.; Wooldridge, P. J.; Bertram, T. H.; Cohen, R. C. *J. Phys. Chem. A* **2005**, *109*, 8520–8525.
- (30) Boxe, C. S.; Colussi, A. J.; Hoffmann, M. R.; Tan, D.; Mastro-marino, J.; Case, A. T.; Sandholm, S. T.; Davis, D. D. *J. Phys. Chem. A* **2003**, *107*, 11409–11413.
- (31) Boxe, C. S.; Colussi, A. J.; Hoffmann, M. R.; Perez, I. M.; Murphy, J. G.; Cohen, R. C. *J. Phys. Chem. A* **2006**, *110*, 3578–3583.
- (32) Watanabe, K.; Ishizaka, Y.; Takenaka, C. *Atmos. Environ.* **2001**, *35*, 645–655.
- (33) Bluhm, H.; Ogletree, D. F.; Fadley, C. S.; Hussain, Z.; Salmeron, M. *J. Phys.: Condens. Matter* **2002**, *14*, L227–L233.
- (34) Kawamura, P. I.; Mackey, D. *J. Hazard. Mater.* **1987**, *15*, 343–364.
- (35) Nair, S. K.; Peters, L. K. *Atmos. Environ.* **1989**, *23*, 1399–1423.
- (36) Brimblecombe, P.; Clegg, S. L.; Khan, I. *J. Aerosol Sci.* **1992**, *23*, S901–S904.
- (37) Khan, I.; Brimblecombe, P. *J. Aerosol Sci.* **1992**, *23*, S897–S900.
- (38) Collett, J., Jr.; Iovinelli, R.; Demoz, B. *Atmos. Environ.* **1995**, *29*, 1145–1154.
- (39) Dubouski, Y.; Colussi, A. J.; Hoffmann, M. R. *J. Phys. Chem. A* **2001**, *105*, 4928–4932.
- (40) Jacobi, H. W.; Hilker, B. *J. Photochem. Photobiol. A* **2007**, *185*, 371–382.
- (41) Rempel, A. W.; Waddington, E. D.; Wettlaufer, J. S.; Worster, M. G. *Nature* **2001**, *411*, 568–571.
- (42) Ikeda-Fukazawa, T.; Fukumizu, K.; Kawamura, K.; Aoki, S.; Nakazawa, T.; Hondoh, T. *Earth Planet. Sci. Lett.* **2005**, *229*, 183–192.
- (43) McCabe, J. R.; Boxe, C. S.; Colussi, A. J.; Hoffmann, M. R.; Thiemens, M. H. *J. Geophys. Res., [Atmos.]* **2005**, *110*; DOI: 10.1029/2004JD005484. JP075551R